Ethanol/Water Mixture Pervaporation Performance of *b*-Oriented Silicalite-1 Membranes Made by Gel-Free Secondary Growth

Bahman Elyassi, Mi Young Jeon, and Michael Tsapatsis
Dept. of Chemical Engineering and Materials Science, University of Minnesota, Minneapolis, MN 55455

Katabathini Narasimharao, Sulaiman Nasir Basahel, and Shaeel Al-Thabaiti
Dept. of Chemistry, Faculty of Science, King Abdulaziz University, Jeddah 21589, Saudi Arabia

DOI 10.1002/aic.15124
Published online December 22, 2015 in Wiley Online Library (wileyonlinelibrary.com)

b-oriented silicalite-1 membranes on porous silica supports were synthesized using gel-free secondary growth. The porous silica supports were made by pressing crushed quartz fibers followed by sintering and polishing, and further modified by slip-coating three layers of Stöber silica particles (1000, 350, and 50 nm). The b-oriented seed layers were prepared by rubbing silicalite-1 particles (2 μm × 0.8 μm × 3 μm along a-, b-, and c-axis, respectively) after depositing a polymeric layer on the support. After silicalite-1 seed deposition, a final coating of spherical silica particles was applied. Well-intergrown, μm-thick, b-oriented membranes were obtained, which, after calcination, exhibited ethanol permselectivity in ethanol/water mixture pervaporation. At 60°C and for ~5 wt % ethanol/water mixtures, the best membrane exhibited overall pervaporation separation factor of 85 (corresponding to membrane intrinsic selectivity of 7.7) and total flux of 2.1 kg/(m^2·h). This performance is comparable to the best performing MFI membranes reported in the literature. *AIChE J*, 62: 556–563, 2016
Keywords: pervaporation, zeolite membrane, silicalite-1, gel-free crystal growth, ethanol

Introduction

Hybrid distillation-vapor permeation is the-state-of-the-art technology for bioethanol separation. The first industrial scale unit was installed in 2000 by Mitsui Engineering and Shipbuilding Co. in Japan.[1] It relies on hydrophilic NaA membranes for dehydration of ethanol-rich output of the distillation unit. However, direct separation of low-concentration-ethanol from the fermentation broth can be energetically more favorable. In this approach, high performance hydrophobic membranes can potentially lower the energy requirement of bioethanol production in, ideally, single stage pervaporation or vapor permeation or in combination with distillation.[2] All-silica zeolite membranes are promising to tackle this challenge. They are commonly made using secondary (seeded) growth or by *in situ* hydrothermal synthesis.[3] In both cases, substrates are immersed in the growth sols or gels under synthesis conditions, which require use and processing of alkaline mixtures containing expensive structure directing agents (SDA), adding to the manufacturing cost.

Among siliceous zeolites, the mordenite framework inverted (MFI) structure (silicalite-1) has been extensively studied for the separation of ethanol from aqueous mixtures.[4] In a recent development, Yoon and coworkers[5] inspired by earlier work indicating the possibility of growing supported zeolite crystals in the absence of a liquid sol or gel using the substrate as silica source[6] demonstrated preparation of high quality oriented MFI membranes by a method called gel-free secondary growth, in which a small quantity of SDA is used and there is no bulk sol or gel in contact with the seeded support.

For making continuous *b*-oriented MFI membranes, Yoon and coworkers first made porous silica supports by compacting Stöber silica particles on which they deposited oriented MFI monolayers by rubbing. They then impregnated the MFI-coated support with an aqueous solution of tetrapropyl ammonium hydroxide (TPAOH) followed by heating in a closed vessel without adding any liquid.

Recently, it was demonstrated that the gel-free secondary growth approach can also be used to make very thin *b*-oriented membranes on porous silica supports[7] and thin films on Si wafers[8] using exfoliated zeolite nanosheets deposited by filtration and Langmuir Schaefer deposition as seed layers, respectively.

In Ref. 7, in place of the Stöber silica supports, which are of low mechanical strength, a new type of mechanically stronger silica porous support was introduced. It was made by first crushing and then pressing commercially available silica fibers, referred to as quartz fibers, followed by sintering and polishing. To smoothen the support surface, several layers of Stöber silica were deposited including a top 50 nm Stöber silica layer that also serves as silica source to grow the zeolite seed layers to continuous films by the gel-free secondary growth method.

b-oriented MFI membranes made by *b*-oriented conventional seed layers[5] and 3-nm thick zeolite nanosheets[7] exhibit excellent performance in xylene and butane isomer separations. However, this gel-free approach has not yet been explored for

Correspondence concerning this article should be addressed to M. Tsapatsis at tsapatsis@umn.edu.

Table 1. Composition of Solutions that upon Mixing Results in the Formation of Stöber Silica

Size	Solution A	Solution B
1 micron	5 mL TEOS	9 mL NH_4OH (28–30 wt %)
	30 mL ethanol	50 mL ethanol
350 nm	22.3 mL TEOS	96.6 g distilled water
	178 mL ethanol	18.9 mL NH_4OH (28–30 wt %)
		16 mL ethanol
50 nm	4.5 mL TEOS	19.3 mL distilled water
	35.6 mL ethanol	0.6 mL NH_4OH (28–30 wt %)

making *b*-oriented ethanol selective silicalite-1 pervaporation membranes for ethanol/water separation. Here, we demonstrate high pervaporation performance using certain modifications of the gel-free approach.

Materials and Method

Quartz support preparation

Quartz fibers (Technical Glass Products, coarse, 9 μm wool) were crushed by pressing at 4 tons over 1 inch die for 60 s. 2 g of crushed fiber were mixed with 0.5 mL of sodium nitrate (as sintering aid) in a methanol solution (2 mg/mL) and then pressed at 4 tons in 22 mm die for 60 s. Supports were heated at 50°C for 4 h, and then at 1100°C for 3 h with a heating/cooling rate of 4°C/min. The supports were polished with silicon carbide sandpaper (P2500, Buehler) and sonicated (Branson 5510R-DTH, 135 W) in distilled water for 5 s and thoroughly rinsed with water (sonication-rinsing was performed for four times) and dried at 150°C before coating of intermediate layers.

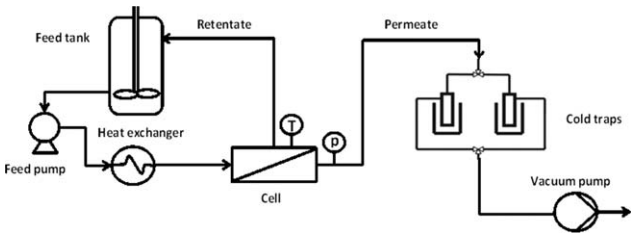

Figure 1. Schematic of the pervaporation experimental set up.

Stöber silica

To form graded intermediate layers on quartz supports, three sizes (1 μm, 350 nm, and 50 nm) of Stöber silica spheres were synthesized. For these syntheses, two solutions, called A and B, were prepared with the compositions given in Table 1.

One micron Stöber silica was synthesized according to the procedure developed by Nozawa et al.[9] Typically, solution A was added to solution B using a syringe pump at a rate of 0.7 mL/h under nitrogen atmosphere. After synthesis, particles were centrifuged at 5,000 rpm for 5 min and washed with 50 mL ethanol for four times. Particles were dried at 70°C overnight and then calcined at 700°C for 4 h.

50 nm and 350 nm silica spheres were synthesized according to the Stöber method.[10] In short, solution A was added to solution B at once and then stirred for 2 h at room temperature. Particles were centrifuged at 12,000 rpm (50 nm) and 10,000 rpm (350 nm) and washed with 50 mL ethanol for four times and then dried overnight at 70°C. 50 nm and 350 nm silica particles were calcined at 400°C and 700°C for 4 h, respectively.

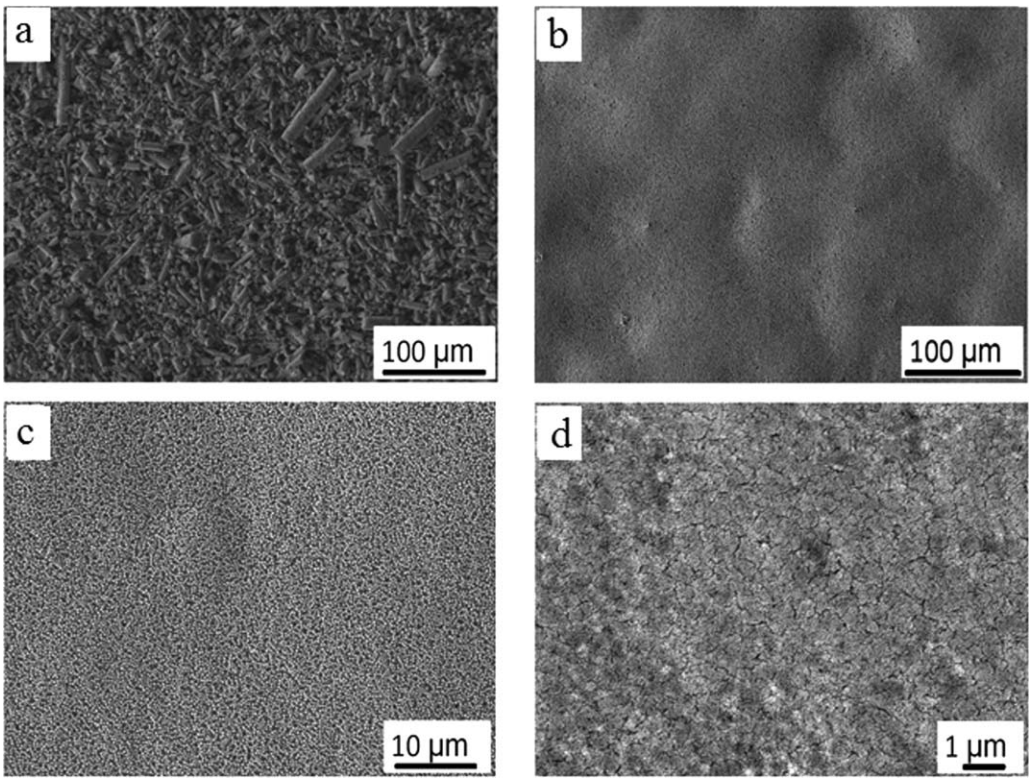

Figure 2. SEM top-view of the bare support (a); after coating with 1 μm Stöber silica (b); 350 nm Stöber silica (c); and 50 nm Stöber silica particles (d).

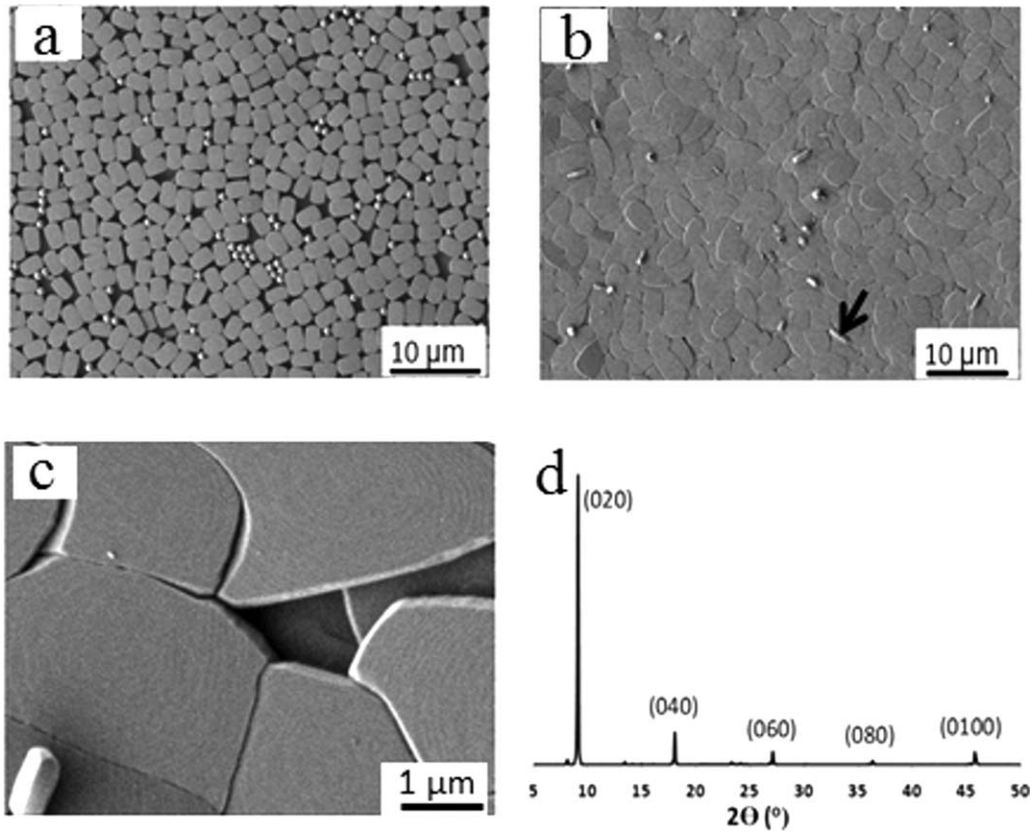

Figure 3. SEM top-view of the seed-coated support (a); the membrane after gel-free secondary growth at low, (b); and high magnification, (c); and the corresponding XRD pattern of the membrane (d). An arrow in (b) points to a twin grain with *a*-out-of-plane orientation.

Stöber silica coatings on quartz supports

0.16 g of 1 micron Stöber silica was dispersed in 4 mL ethanol and sonicated for 1.5 h. Unlike our earlier work,[7] here, a slip-coating method was adopted,[11] in which the support is brought into contact on one side with the Stöber silica suspension for 15 s and then detached gently from the suspension surface on a pendulum's trajectory move. The slip-coated supports were sintered by heating at 50°C for 4 h (heating rate: 1°C/min), 1,020°C for 3 h (heating rate: 2°C/min) and then cooled (cooling rate: 4°C/min).

The following preparation procedures were developed for preparing and then coating the 350 and 50 nm Stöber silica suspensions.

0.2 g of 350 nm Stöber silica was suspended in 50 μL NH_4OH (Sigma-Aldrich, 28–30 wt %) in 20 mL water solution and sonicated for 1.5 h. The suspension was centrifuged at 2,000 rpm for 2 min and the top 15 mL of the solution were carefully removed, centrifuged at 10,000 rpm for 20 min and washed with 50 mL ethanol for three times. Finally, the cake was dispersed in 4 mL ethanol by sonication and filtered through 5 μm and then 2 μm syringe filters.

The porous quartz support coated with 1 μm silica was slip-coated with the 350 nm sol for 12 s and sintered at 50°C for 4 h (heating rate: 1°C/min), 1,020°C for 3 h (heating rate: 2°C/min) and then cooled (cooling rate: 4°C/min).

For 50 nm Stöber silica, the same preparation procedure as for 350 nm particles was used. However, further purification was applied, in which the cake formed after centrifugation was dispersed in 20 mL ethanol and sonicated (Qsonica Q500) for 3 min and then centrifuged at 5,000 rpm for 5 min. The top 15 mL of the sol were separated and filtered through a 0.45 μm syringe filter. The final filtrate volume was increased to 20 mL with addition of ethanol.

Quartz supports coated with 1 μm and 350 nm silica were coated with the 50 nm sol for 8 s and calcined at 50°C for 4 h (heating rate: 1°C/min), 550°C for 6 h (heating rate: 1°C/min) and then cooled (cooling rate: 2°C/min).

Table 2. Pervaporation Performance of *b*-oriented Membranes for a Feed of ~5 wt % Ethanol in Water at 60°C

Membranes	Total Flux (kg/(m^2·h))	S.F. (α_{pervap})	Membrane Selectivity (α_{mem})
24 h Secondary growth at 180°C			
	2.3	76	7.0
	3.5	35	3.2
	3.2	40	3.6
	2.9	39	3.5
30 h Secondary growth at 180°C			
	2.1	85	7.7

b-oriented seed deposition by rubbing

Silicalite-1 seeds were synthesized according to well-established methods.[12,13] Briefly, 10.1 g of TEOS (Sigma-Aldrich, >99%) was added to a solution of 3.69 g TPAOH (Alfa Aesar, 40 wt %) in 87.8 g distilled water and stirred for one day. The clear solution was filtered through paper filter (Fisherbrand^{TM}, P8 grade) and then autoclaved at 150°C under rotation for 12 h. The coffin shape silicalite-1 product was

Table 3. Performance Summary of the Silicalite-1 Membranes for Ethanol/Water Pervaporation Reported in the Literature and in this Work

Membrane (Si/Al)/Support with Pore Size	Method	T (°C)	Ethanol Conc. in Feed (wt%)	Separation Factor (α_{pervap})	Membrane Selectivity[a] (α_{mem})	Flux kg/(m^2·h)	Orientation	Ref.
B-ZSM-5 (Si/B ≈ 97.5)/γ-Alumina/α-Alumina/SiC monoliths (CeraMem Corp.) 5 nm top layer	*In situ*	60	5	31	**2.9**[b]	0.2	N/A	17
Silicalite-1 (∞)/α-Alumina tube (Foshan ceramics research institute) 2–3 μm	Secondary	60	5	45	**4.1**	1.4	N/A	18
				39	**3.6**	1.5	N/A	
Silicalite-1 (∞)/mullite tube 1 μm	*In situ*	60	5	106	**9.8**	0.9	*r*	19
	Secondary			65	**6**	1.3	N/A	
Silicalite-1 (∞)/α-Alumina tube 1 μm	*In situ*	60	5	85	**7.8**	1.2	N/A	
Silicalite-1 (∞)/mullite tube 1 μm	Secondary	60	5	62	**5.7**	2.2	N/A	20
				72	**6.6**	1.4	N/A	
Silicalite-1 (∞)/α-Alumina tube 2 μm	Secondary	60	5	89	**8.2**	1.8	N/A	
Silicalite-1 (∞)/stainless steel tube 0.1 μm	Secondary	60	5	30	**2.8**	4.0	N/A	
				35	**3.2**	3.7	N/A	
Silicalite-1 (∞)/stainless steel disc 10 μm	*In situ*	30	4.65	64	**6.1**	0.6	*r*	21
Silicalite-1 (∞)/stainless steel disc 10 μm	*In situ*	30	4.95	43	**4.1**	0.4	*r*	22
Silicalite-1 (∞)/stainless steel disc 0.5–2 μm	*In situ*	60	4	58	**5.2**	0.8	*r*	23
Silicalite-1 (∞)/α-Alumina disc 0.5–2 μm	*In situ*	30	4	65	**6.0**	0.1	*r*	
Silicalite-1 (∞)/stainless steel disc 2 μm	*In situ*	30	4	63	**5.9**	0.6	*r*	24
Silicalite-1 (∞)/stainless steel disc 0.5–2 μm	*In situ*	30	4	32	**3.0**	0.7	*r*	25
				42	**3.9**	0.5		
Silicalite-1 (∞)/stainless steel disc 2 μm	*In situ*	30	4	47	**4.4**	0.4	N/A	26
				26	**2.4**	0.3		
Silicalite-1 (∞)/silica tube 0.3 μm	*In situ*	80	3	66	**5.7**	1.5	N/A	27
				72	**6.2**	1.1	N/A	
Silicalite-1 (∞)/α-Alumina tube 0.3 μm	*In situ*	80	3	32	**2.8**	0.5	N/A	
Silicalite-1 (∞)/stainless steel tube (Mott Corp.) 0.5 μm	*In situ*	25	5	10	**1.0**	0.1	N/A	28
Ge-ZSM5 (Si/Ge ≈ 100)/stainless steel tube (Mott Corp.) 0.5 μm	*In situ*	25	5	29	**2.8**	0.1	N/A	
Silicalite-1 (∞)/α-Alumina monolith (NGK Insulators)	N/A	76	16	39	**4.6**	1.9	N/A	29
		76	16	41	**4.8**	1.1		
		76	7.3	31	**2.9**	1.5		
		104	16	22	**2.7**	4.3		
Silicalite-1 (∞)/α-Alumina tubes (Hyflux CEPAraction Technologies) 0.2 μm	Secondary	45	5	33	**3.1**	0.7	N/A	30
		45	5	51	**4.8**	1.5	*c*	
		65	5	45	**4.2**	2.3		
Silicalite-1 (∞)/α-Alumina tubes (Hyflux CEPAraction Technologies) 0.8 μm	Secondary	45	5	40	**3.8**	1.1	N/A	
				54	**5.1**	1.5	*c*	
Silicalite-1 (∞)/α-Alumina tubes (Pall Exekia) 0.2 μm top layer	Secondary	25	5	43	**4.1**	0.2	*r*	31
				36	**3.5**	1.0		
				22	**2.1**	1.6		
Silicalite-1 (∞)/mullite tubes (Nikkato Corp.) 1.9 μm	Secondary	60	3.7	36	**3.3**	0.7	N/A	32
			10	16	**1.6**	0.7		
ZSM-5 (Si/Al ≈ 300)/titania tubes (Nikkato Corp.) 34 nm top layer	Secondary	60	5	~81	**7.5**	~1.8	N/A	33
Silicalite-1 (∞)/stainless steel tubes (Pall Corp.) 1 μm	Secondary	60	5	23	**2.1**	1	c/h0h	34
				43	**4.0**	1.2		
Silicalite-1 (∞)/stainless steel tube 0.2 μm	Secondary	30	5	~60	**5.7**	~0.2	N/A	35
Silicalite-1 (∞)/Mullite tube (Nikkato Corp.) 1 μm	Secondary	60	5	60	**5.5**	2.9	(0 1 1) (1 0 1)	36

TABLE 3. *Continued*

Membrane (Si/Al)/Support with Pore Size	Method	T (°C)	Ethanol Conc. in Feed (wt%)	Separation Factor (α_{pervap})	Membrane Selectivity[a] (α_{mem})	Flux kg/(m^2.h)	Orientation	Ref.
Silicalite-1 (∞)/stainless-steel net support (300 mesh)	Secondary	25	5	20	**1.9**	11.5	*c*	37
Silicalite-1 (∞)/YSZ fiber 0.67 μm	Secondary	60	5	47	**4.3**	7.4	N/A	38
Silicalite-1 (∞)/α-Alumina hollow fiber 100-200 nm	Secondary	60	3	66	**5.8**	2.9	h0h/oblique *c*	39
Silicalite-1 (∞)/α-Alumina tube 1–3 μm	Secondary	60	5	62	**5.7**	1.8	N/A	40
Silicalite-1 (∞)/α-Alumina disc (Fraunhofer IKTS, Germany) 100 nm top layer	Secondary	60	10	4	**0.4**	10.7	N/A	41
MFI/α-Alumina tube 1–3 μm	Secondary	60	5	88	**8.1**	1.2	N/A	42
Silicalite-1 (∞)/silica tube 0.3 μm	*In situ*	60	3	95	**8.4**	0.6	N/A	43
Silicalite-1 (∞)/mullite tube (Nikkato Corp.) 1.0 μm	Secondary	60	5	66	**6.1**	1.9	011	44
MFI/α-Alumina disc (Fraunhofer IKTS, Germany) 100 nm top layer	Secondary	110	10	5	**0.5**	51.6	N/A	45
Silicalite-1 (∞)/porous silica disc (quartz + Stöber)	Gel-free	60	4.3-5	85	**7.7**	2.1	*b*	This work

[a]Intrinsic membrane selectivity (α_{mem}) is determined using Eq. 3, the reported α_{pervap} and calculated α_{evap} from NRTL model in Aspen Plus V8.0.
[b]Bold indicates the quantity (membrane selectivity) calculated.

Figure 4. Plot of performances from Table 2 based on $\alpha_{mem}-1$ vs. total flux. Feed conditions of 5 wt % ethanol and 60°C (○: literature; ●: this work). Feed conditions other than 5 wt % ethanol and 60°C (Δ: literature; ▲: this work with feed condition of 5 wt % ethanol and 75°C).

[Color figure can be viewed in the online issue, which is available at wileyonlinelibrary.com.]

washed with water and centrifuged repeatedly until pH = 7 was reached.

After synthesis, the seeds were vacuum freeze dried. To rub seeds on the Stöber silica coated porous quartz support, a suitable polymeric intermediate layer was required. Otherwise, during rubbing seeds slip on the support due to weak adhesion. The following procedure was used to form a polymeric intermediate layer between support and seeds. First, a 50 wt % solution of polyacrylic acid (Sigma-Aldrich, Mw 1800) in water was prepared and sonicated for 1 h. Then, 0.2 mL ethylene glycol was added to 1 mL solution of polyacrylic acid and the solution was degassed by sonication for 20 min. The solution was spin-coated at 4,000 rpm for 15 s on the quartz support and then heated at 70°C in a convection oven for 1 h. This procedure was repeated for one additional time to make sure the polymeric film covers the entire surface of the support.

Silicalite-1 seeds were rubbed by hand using Sterling Nitrile powder-free gloves very gently on the polymer coated-support, followed by drying at 150°C for 1 min. Then, 1 μm spherical silica powder (Alfa Aesar) was rubbed over the seeds using latex powder-free (Premium Touch Gold Grip Plus) gloves.

The seeded supports prepared as described above were calcined at 550°C for 6 h (heating rate: 1°C/min) and then cooled (cooling rate: 2°C/min) to decompose the polymeric layer and fix the seeds on the support.

Gel-free secondary growth

Seeded supports were coated on one side with equimolar solution (0.075 M) of tetrapropyl ammonium bromide (TPABr, Sigma-Aldrich, 98%) and KOH (potassium hydroxide, Sigma-Aldrich, 85%) for 20 s and then immediately autoclaved at 180°C without adding any liquid. Growth times were 24 and 30 h. The membranes were removed from the autoclaves, rinsed with water, dried at 70°C for 2 h, and then

Table 4. Selected High-Performance Membranes Reported in the Literature

Synthesis Conditions	Compositions	Support	α_{pervap}	Flux kg/(m^2·h)	Ref.
In situ growth (16 h)	SiO_2:TPAOH:H_2O	Silicalite-1 (∞)/mullite tube,	106	0.9	19
Synthesis temperature (175°C)	1:0.17:120	pore size 1 μm (membrane	85	1.2	
In situ growth (24 h)		thickness 15-20 μm)			
Synthesis temperature (185°C)		Silicalite-1 (∞)/α-Alumina tube, pore size 2 μm (membrane thickness ~10 μm)			
Secondary growth (5.5 h)	SiO_2:TPAOH:H_2O	Silicalite-1 (∞)/α-Alumina tube,	89	1.8	20
Synthesis temperature (185°C)	0.17:1:120	pore size 2 μm (membrane thickness > 17 μm)			
Secondary growth	SiO_2:Al_2O_3:NaOH:TPABr:	ZSM-5 (Si/Al ≈ 300)/titania tube	81	1.8	33
Synthesis temperature (180°C)	H_2O 1:0.00166:0.035:0.0035:85	(Nikkato Corp.) with top layer of 34 nm pores (membrane thickness 50 μm)			
Secondary growth (16 h)	TEOS:NaOH:TPAOH:H_2O	MFI/α-Alumina tube 1–3 μm	88	1.2	42
Synthesis temperature (175°C)	1:0.095:0.005:165	(membrane thickness N/A)			

calcined at 400°C for 12 h (heating rate: 1°C/min, cooling rate: 1.5°C/min).

Pervaporation experiments

A schematic of the pervaporation setup is presented in Figure 1. The feed temperature was controlled by circulating fluid through a heat exchanger, which was heated by a Lauda–Brinkman ECO thermostat. Two liquid nitrogen cold traps in parallel were used to collect permeate condensates. The permeate was weighed and its composition was analyzed by a gas chromatograph (Agilent Technologies 7890N) equipped with a thermal conductivity detector (TCD) and a capillary column (DB-624).

The performance of the membranes was investigated using a feed of ~5 wt % ethanol/water solution at 60°C and other temperatures.

The overall ethanol-water pervaporation separation factor, α_{pervap}, and total flux J (kg/(m^2·h)) are defined, respectively, as

$$\alpha_{pervap} = \frac{m_{ethanol,p} / m_{water,p}}{m_{ethanol,f} / m_{water,f}} \quad (1)$$

$$J = M / (A \times t) \quad (2)$$

where, $m_{i,p}$ and $m_{i,f}$ are the mass fractions of component i (water or ethanol) in the permeate and feed, respectively, M is the total permeate (in kg) collected after time t (in hours) and A is the surface area of the membrane in m^2.

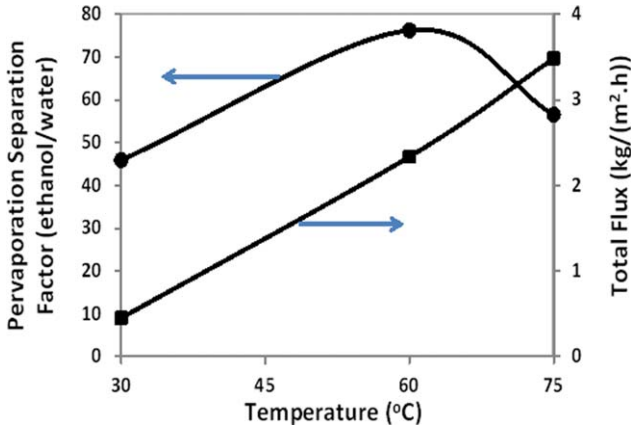

Figure 5. Effect of temperature on the performance of *b*-oriented membranes (membrane grown for 24 h at 180°C).

[Color figure can be viewed in the online issue, which is available at wileyonlinelibrary.com.]

The above definition of pervaporation separation factor, commonly reported in the literature, can be further broken down into two terms to distinguish between evaporation separation factor and intrinsic membrane selectivity as[14–16]

$$\alpha_{pervap} = \alpha_{evap} \times \alpha_{mem} \quad (3)$$

The evaporation separation factor, α_{evap}, is a function of feed conditions and can be readily obtained from the vapor–liquid equilibrium data and the following equation

$$\alpha_{evap} = \frac{m_{ethanol,v} / m_{water,v}}{m_{ethanol,f} / m_{water,f}} \quad (4)$$

where, $m_{i,v}$ is the mass fraction of component i (ethanol or water) in the vapor phase in equilibrium with the feed in liquid state. We have used NRTL model in Aspen Plus V8.0 to calculate α_{evap}.

α_{mem} calculated by the above procedure is the same as that calculated from the ratio of molar permeances:

$$\alpha_{mem} = \frac{P_{ethanol}}{P_{water}}$$

with $P_{ethanol} = \frac{Q_{ethanol}}{p_{ethanol,v} - p_{ethanol,p}}$ and $P_{water} = \frac{Q_{water}}{p_{water,v} - p_{water,p}}$

where, $p_{i,v}$ is the vapor pressure for each component in equilibrium with the feed liquid and $p_{i,p}$ is the partial pressure for each component in the permeate side, assumed to be negligible compared to that in the feed ($p_{ethanol,v} \gg p_{ethanol,p}$ and $p_{water,v} \gg p_{water,p}$).

Results and Discussion

Figure 2 shows scanning electron microscopy (SEM) top-view images of the bare support and the subsequent Stöber silica intermediate layers. For continuous seed layer formation on the substrate by rubbing method, smoothness of the substrate is of critical importance. The quality of the Stöber silica layers formed here by slip-coating is comparable to that of the layers reported earlier and made by rubbing.[7] The current approach is advantageous as it allows for easier scale up and removes the uncertainties introduced by the rubbing approach. Figure 3 shows top-view SEM images of *b*-oriented out-of-plane seeded supports before (Figure 3a) and after (Figure 3b and c) gel-free secondary growth with the corresponding X-ray diffraction (XRD) pattern after secondary growth (Figure 3d).

Spherical silica particles are evident in Figure 3a in between the silicalite-1 seeds. They are placed there by the final rubbing step after seed layer formation. SEM top views of the membranes after secondary growth indicate high degree of intergrowth and preservation of the preferred orientation of the seeds with only a small occurrence of twinning at grain boundaries. The higher magnification top-view SEM shown in Figure 3c indicates grain overlapping in areas of reduced film thickness. This is a desirable characteristic to reduce nonselective transport pathways and it appears to be a result of gel-free secondary growth where nutrients for crystal growth are being made available from below the seed layer and not from the top as in conventional sol-based secondary growth. The XRD pattern indicates high degree of *b*-out-of-plane orientation and cross-section SEM (not shown) indicates a membrane thickness of 1.5 μm.

Membrane pervaporation performances are shown in Table 2. *b*-oriented membrane after 30 h secondary growth showed higher selectivity and lower flux than membranes grown for 24 h. Membranes with α_{pervap} of 85 and high flux of 2.1 kg/(m^2 h) can be prepared. We found that if the last step of silica coating (applied after the deposition of zeolite seeds) is omitted, membrane quality is not consistent. It appears that its use allows the consistent formation of a monolayer of seeds on the substrate.

To compare the membranes made in this work with those reported in the literature, a summary of the performance of silicalite-1 membranes is presented in Table 3 and plotted in Figure 4. As can be seen, the *b*-oriented membranes made in this work are comparable to the best reported silicalite-1 membranes in the literature, if both selectivity and flux are taken into account. High performance MFI membranes tested under the same conditions used herein are presented in Table 4. Considering the differences in thickness, aluminum content, support used, and microstructure, it is not possible to interpret the similarities in flux and selectivity performance in terms of common desirable characteristics. Most striking are the small differences in flux despite the more than order of magnitude differences in thickness (e.g., 50 μm in Ref. 18 vs. 1.5 μm of the membranes reported here). It is likely that support transport resistances affect the performance of the thin membranes and mask the differences in intrinsic performance of the zeolite membrane layers.

The performance of a *b*-oriented membrane at different temperatures is exhibited in Figure 5. The flux increased to as high as 3.5 kg/(m^2·h) at 75°C at the cost of reduction in the separation factor to approximately 60.

This high performance, along with the advantages of the gel-free approach for easy and reproducible scale up and for reduced cost, make this approach very promising and worthy of further investigations aiming to improved membrane quality and performance.

Conclusion

Fabrication of *b*-oriented silcialite-1 membranes on porous silica supports via gel-free secondary growth for ethanol/water mixture pervaporation was demonstrated for the first time. The performance of the 30 h grown membranes is comparable to the best reported in the literature. The pervaporation separation factor was as high as 85, corresponding to membrane intrinsic selectivity of 7.7, and the total flux was 2.1 kg/(m^2·h).

Acknowledgments

Financial support for the membrane characterization was provided by the Deanship of Scientific Research at the King Abdulaziz University D-003/433. Funds for membrane synthesis were provided by the Department of Energy's ARPA-E program (Award number DE-AR0000338 (0670-3240)). M.T. acknowledges the generous support provided by the Amundson Chair fund at the University of Minnesota. Parts of this work were conducted at the Characterization Facility at the University of Minnesota, which receives partial support from the NSF through the MRSEC program.

Literature Cited

1. Gascon J, Kapteijn F, Zornoza B, Sebastian V, Casado C, Coronas J. Practical approach to zeolitic membranes and coatings: state of the art, opportunities, barriers, and future perspectives. *Chem Mater*. 2012;24(15):2829–2844.
2. Kelloway A, Tsapatsis M, Daoutidis P. Techno-economic analysis of ethanol-selective membranes for corn ethanol-water separation. In: 12th International Symposium on Process Systems Engineering and 25th European Symposium on Computer Aided Process Engineering. Copenhagen: Denmark, 2015.
3. Rangnekar N, Mittal N, Elyassi B, Caro J, Tsapatsis M. Zeolite membranes - a review and comparison with MOFs. *Chem Soc Rev*. 2015;44(20):7128–7154.
4. Xia S, Peng Y, Wang Z. Microstructure manipulation of MFI-type zeolite membranes on hollow fibers for ethanol–water separation. *J Membr Sci*. 2016;498:324–335.
5. Pham TCT, Nguyen TH, Yoon KB. Gel-free secondary growth of uniformly oriented silica MFI zeolite films and application for xylene separation. *Angew Chem Int Edit*. 2013;52(33):8693–8698.
6. Chaikittisilp W, Davis ME, Okubo T. TPA^+-mediated conversion of silicon wafer into preferentially-oriented MFI zeolite film under steaming. *Chem Mater*. 2007;19(17):4120–4122.
7. Agrawal KV, Topuz B, Pham TCT, Nguyen TH, Sauer N, Rangnekar N, Zhang H, Narasimharao K, Basahel SN, Francis LF, Macosko CW, Al-Thabaiti S, Tsapatsis M, Yoon KB. Oriented MFI membranes by gel-less secondary growth of sub-100 nm MFI-nanosheet seed layers. *Adv Mater*. 2015;27(21):3243–3249.
8. Rangnekar N, Shete M, Agrawal KV, Topuz B, Kumar P, Guo Q, Ismail I, Alyoubi A, Basahel S, Narasimharao K, Macosko CW, Mkhoyan KA, Al-Thabaiti S, Stottrup B, Tsapatsis M. 2D zeolite coatings: langmuir–schaefer deposition of 3 nm thick mfi zeolite nanosheets. *Angew Chem*. 2015;127(22):6671–6675.
9. Nozawa K, Gailhanou H, Raison L, Panizza P, Ushiki H, Sellier E, Delville JP, Delville MH. Smart control of monodisperse Stober silica particles: effect of reactant addition rate on growth process. *Langmuir*. 2005;21(4):1516–1523.
10. Stöber W, Fink A, Bohn E. Controlled growth of monodisperse silica spheres in the micron size range. *J. Colloid Interface Sci*. 1968;26(1):62–69.
11. Leenaars AFM, Burggraaf AJ. The preparation and characterization of alumina membranes with ultrafine pores. 2. The formation of supported membranes. *J Colloid Interface Sci*. 1985;105(1):27–40.
12. Pham TCT, Kim HS, Yoon KB. Growth of uniformly oriented silica MFI and BEA zeolite films on substrates. *Science*. 2011;334(6062):1533–1538.
13. Zhou M, Hedlund J. Oriented monolayers of submicron crystals by dynamic interfacial assembly. *J Mater Chem*. 2012;22(8):3307–3310.
14. Paradis GG, Shanahan DP, Kreiter R, van Veen HM, Castricum HL, Nijmeijer A, Vente JF. From hydrophilic to hydrophobic HybSi (R) membranes: a change of affinity and applicability. *J Membr Sci*. 2013;428:157–162.
15. Wijmans JG, Baker RW. A simple predictive treatment of the permeation process in pervaporation. *J Membr Sci*. 1993;79(1):101–113.
16. Sommer S, Melin T. Performance evaluation of microporous inorganic membranes in the dehydration of industrial solvents. *Chem Eng Process*. 2005;44(10):1138–1156.
17. Bowen TC, Kalipcilar H, Falconer JL, Noble RD. Pervaporation of organic/water mixtures through B-ZSM-5 zeolite membranes on monolith supports. *J Membr Sci*. 2003;215(1-2):235–247.
18. Shen D, Xiao W, Yang J, Chu N, Lu J, Yin D, Wang J. Synthesis of silicalite-1 membrane with two silicon source by secondary growth

method and its pervaporation performance. *Sep Purif Technol*. 2011; 76(3):308–315.
19. Lin X, Chen X, Kita H, Okamoto K. Synthesis of silicalite tubular membranes by in situ crystallization. *AIChE J*. 2003;49(1):237–247.
20. Lin X, Kita H, Okamoto K-I. Silicalite membrane preparation, characterization, and separation performance. *Ind Eng Chem Res*. 2001; 40(19):4069–4078.
21. Nomura M, Yamaguchi T, Nakao S-I. Ethanol/water transport through silicalite membranes. *J Membr Sci*. 1998;144(1-2):161–171.
22. Nomura M, Yamaguchi T, Nakao S-I. Transport phenomena through intercrystalline and intracrystalline pathways of silicalite zeolite membranes. *J Membr Sci*. 2001;187(1-2):203–212.
23. Sano T, Yanagishita H, Kiyozumi Y, Mizukami F, Haraya K. Separation of ethanol-water mixture by silicalite membrane on pervaporation. *J Membr Sci*. 1994;95(3):221–228.
24. Sano T, Hasegawa M, Kawakami Y, Yanagishita H. Separation of methanol/methyl-tert-butyl ether mixture by pervaporation using silicalite membrane. *J Membr Sci*. 1995;107(1-2):193–196.
25. Ikegami T, Yanagishita H, Kitamoto D, Haraya K, Nakane T, Matsuda H, Koura N, Sano T. Production of highly concentrated ethanol in a coupled fermentation/pervaporation process using silicalite membranes. *Biotechnol Tech*. 1997;11(12):921–924.
26. Matsuda H, Yanagishita H, Negishi H, Kitamoto D, Ikegami T, Haraya K, Nakane T, Idemoto Y, Koura N, Sano T. Improvement of ethanol selectivity of silicalite membrane in pervaporation by silicone rubber coating. *J Membr Sci*. 2002;210(2):433–437.
27. Chen HL, Li YS, Yang WS. Preparation of silicalite-1 membrane by solution-filling method and its alcohol extraction properties. *J Membr Sci*. 2007;296(1-2):122–130.
28. Tuan VA, Li SG, Falconer JL, Noble RD. Separating organics from water by pervaporation with isomorphously-substituted MFI zeolite membranes. *J Membr Sci*. 2002;196(1):111–123.
29. Kuhn J, Sutanto S, Gascon J, Gross J, Kapteijn F. Performance and stability of multi-channel MFI zeolite membranes detemplated by calcination and ozonication in ethanol/water pervaporation. *J Membr Sci*. 2009;339(1-2):261–274.
30. Sebastian V, Mallada R, Coronas J, Julbe A, Terpstra RA, Dirrix RWJ. Microwave-assisted hydrothermal rapid synthesis of capillary MFI-type zeolite-ceramic membranes for pervaporation application. *J Membr Sci*. 2010;355(1-2):28–35.
31. Soydas B, Dede O, Culfaz A, Kalipcilar H. Separation of gas and organic/water mixtures by MFI type zeolite membranes synthesized in a flow system. *Microporous Mesoporous Mater*. 2010;127(1-2):96–103.
32. Hasegawa Y, Kimura K, Nemoto Y, Nagase T, Kiyozumi Y, Nishide T, Mizukami F. Real-time monitoring of permeation properties through polycrystalline MFI-type zeolite membranes during pervaporation using mass-spectrometry. *Sep Purif Technol*. 2008;58(3): 386–392.
33. Weyd M, Richter H, Puhlfurss P, Voigt I, Hamel C, Seidel-Morgenstern A. Transport of binary water-ethanol mixtures through a multilayer hydrophobic zeolite membrane. *J Membr Sci*. 2008;307(2):239–248.
34. Stoeger JA, Choi J, Tsapatsis M. Rapid thermal processing and separation performance of columnar MFI membranes on porous stainless steel tubes. *Energy Environ Sci*. 2011;4(9):3479–3486.
35. Sakaki K, Habe H, Negishi H, Ikegami T. Pervaporation of aqueous dilute 1-butanol, 2-propanol, ethanol and acetone using a tubular silicalite membrane. *Desalin Water Treat*. 2011;34(1–3):290–294.
36. Zhang X, Zhu M, Zhou R, Chen X, Kita H. Synthesis of silicalite-1 membranes with high ethanol permeation in ultradilute solution containing fluoride. *Sep Purif Technol*. 2011;81(3):480–484.
37. Zou X, Bazin P, Zhang F, Zhu G, Valtchev V, Mintova S. Ethanol recovery from water using silicalite-1 membrane: an operando infrared spectroscopic study. *Chempluschem*. 2012;77(6):437–444.
38. Shu X, Wang X, Kong Q, Gu X, Xu N. High-flux MFI zeolite membrane supported on YSZ hollow fiber for separation of ethanol/water. *Ind Eng Chem Res*. 2012;51(37):12073–12080.
39. Shan L, Shao J, Wang Z, Yan Y. Preparation of zeolite MFI membranes on alumina hollow fibers with high flux for pervaporation. *J Membr Sci*. 2011;378(1–2):319–329.
40. Peng Y, Zhan Z, Shan L, Li X, Wang Z, Yan Y. Preparation of zeolite MFI membranes on defective macroporous alumina supports by a novel wetting-rubbing seeding method: role of wetting agent. *J Membr Sci*. 2013;444:60–69.
41. Korelskiy D, Leppajarvi T, Zhou H, Grahn M, Tanskanen J, Hedlund J. High flux MFI membranes for pervaporation. *J Membr Sci*. 2013;427:381–389.
42. Peng Y, Lu H, Wang Z, Yan Y. Microstructural optimization of MFI-type zeolite membranes for ethanol-water separation. *J Mater Chem A*. 2014;2(38):16093–16100.
43. Chen H, Song C, Yang W. Effects of aging on the synthesis and performance of silicalite membranes on silica tubes without seeding. *Microporous Mesoporous Mater*. 2007;102(1-3):249–257.
44. Zhang X-L, Zhu M-H, Zhou R-F, Chen X-S, Kita H. Synthesis of a silicalite zeolite membrane in ultradilute solution and its highly selective separation of organic/water mixtures. *Ind Eng Chem Res*. 2012;51(35):11499–11508.
45. Yu L, Korelskiy D, Grahn M, Hedlund J. Very high flux MFI membranes for alcohol recovery via pervaporation at high temperature and pressure. *Sep Purif Technol*. 2015;153:138–145.

Manuscript received Sep. 25, 2015, and revision received Nov. 18, 2015.